SIS100 DIPOLE FIELD HARMONICS AND DYNAMIC APERTURE CALCULATIONS

C. Omet, E. Fischer, G. Franchetti, V. Kornilov, A. Mierau, C. Roux, D. Schäfer, P. Schnizer,
S. Sorge, P. Spiller, K. Sugita
GSI, Darmstadt, Germany

Abstract

During the acceptance test of the First of Series (FoS) SIS100 superferric dipole magnet, detailed field measurements have been done. The harmonic coefficients have been extracted from these and dynamic aperture simulations have been done which are presented here. Furthermore, geometric precision measurement tools for the magnet have been developed to track down the field errors to geometric errors. Finally, mitigation actions have been taken to reduce these errors during manufacturing to ensure the design beam survival rate in SIS100.

SIS100 FOS DIPOLE PERFORMANCE

The SIS100 dipole magnet is a 3 m long super-ferric, curved magnet, see Fig. 1. It is the end of a successful development [1–4] and the first magnet with a high current coil made from Nuclotron cable and cooled by forced-flow 4.5 K two-phase He. It has a maximum field of 1.9 T and will be used at a very high ramp rate of up to 4 T/s in FAIR's driver synchrotron, SIS100. The gap size is 143 mm × 68 mm.
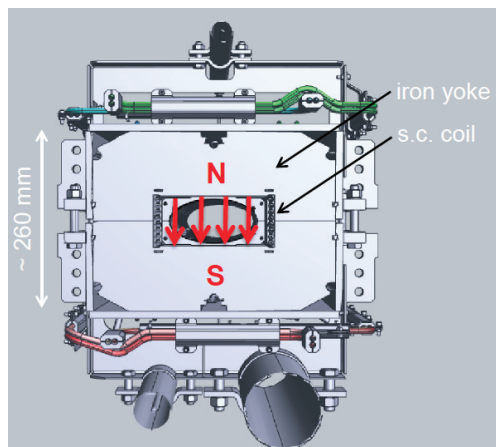
Figure 1: Cross section of the SIS100 dipole.

The First of Series (FoS) SIS100 dipole was delivered 2013 [5, 6] and has been thoroughly tested both at warm and cold conditions in the prototype test facility at GSI. Tests included electrical, geometrical, thermal checks and finally quench training and magnetic field measurements. The nominal current of 13.1 kA has been exceeded already after the second quench; even after several (8) thermal cycles, the magnet did not show a de-training behavior. AC losses at maximum ramp rate and triangular cycle have been measured to be 51 W, which is ≈30% below the calculated value and gives extra margin for the cryogenic plant of FAIR.

Beam stability during the 1 s long bunch-to-bucket injection from SIS18 into SIS100 has to be ensured. This poses a restriction onto the maximum allowable field errors of the magnets. For the dipoles, at injection field of 0.27 T (I = 1.5 kA), the good field region is 115 x 60 mm^2, where a field homogeneity of $\Delta B/B_0 \leq \pm 6 \times 10^{-4}$ is tolerated by design. Furthermore, it is important to have stable beams during middle to high energies at an up to 10 s long slow extraction plateau from SIS100 to the experiments, too.

Field Harmonics

The measurement campaign of the SIS100 dipole was based on the methods described in [7–10]. The following measurement systems were used:

- a single stretched wire system,

- a hall probe system,

- and a rotating coil probe system with transverse translated fields.

The last method allows deriving harmonics up to the 7th order reliably [6]. These measured data has been cross checked with a hall probe mapper and was proven to match. The analysis of these results, recalculated to a reference radius of 40 mm is shown in Fig. 2. Not allowed harmonics are larger than the allowed ones, which was somehow surprising and lead to detailed investigations of the magnet. In particular, the skew quadrupole is large.

To be useful for beam dynamics calculations, the harmonics have been re-calculated to be a valid expansion around the reference orbit, not the rotating coil probe axis.

Geometry Measurements

As for the magnet's super-ferric design, its magnetic field is dominated by the yoke's gap geometry. To track down the measured field errors to their probable root causes, the yoke geometry was measured very precisely. Therefore, special mechanical and capacitive measurement devices have been developed which are able to measure the gap height and width with a precision of ±10 μm in both warm and cold conditions. The measurements have been calibrated and cross checked with laser tracker measurements and found to be consistent.

The results of the gap height measurements along the magnet axis are shown in Fig. 3. The gap height is nonuniform along the magnet by ≈200 μm; the gap height between left and right side (parallelism) differs by ≈80 μm. As it will

7: Accelerator Technology

T10 - Superconducting Magnets

(a) b_2

(b) a_2

(c) b_3

(d) a_3
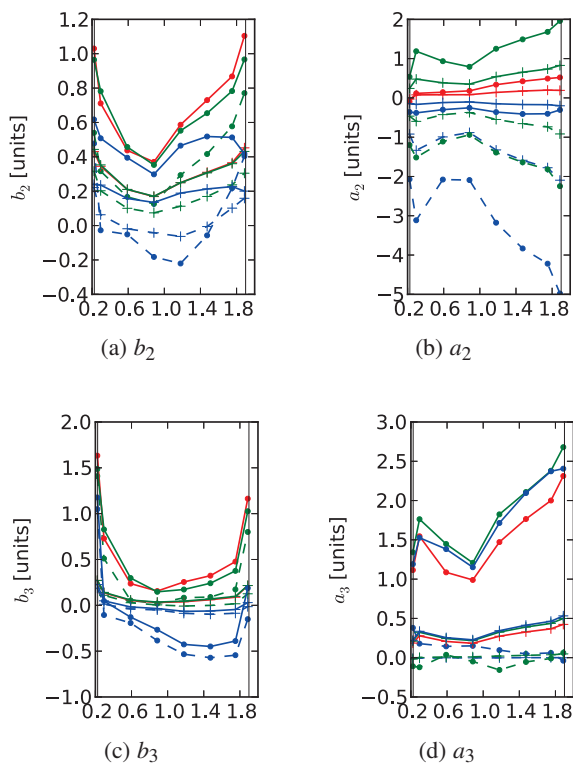
Figure 2: Low order allowed (b_3) and not allowed (a_2, b_2, a_3) measured harmonics within the central field region. Blue dashed z=-900, green dashed z=-300, red solid z=0, green solid z=+300, blue solid z=+900 mm. "+" central coil probe pos. only, "." combined from all three coil probe positions.
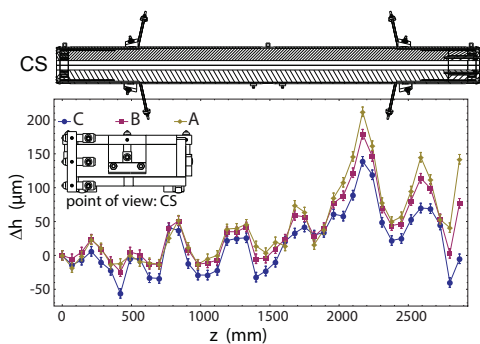
Figure 3: Measured gap height. CS=Cable Connection Side.

be shown below, this in turn creates both normal and skew quadrupole errors.

As dismounting the magnet's coil was not feasible at that time, only the window between the coil was measured, see Fig. 4. Here, width variations larger than 200 μm have been observed at two distinct points in the vicinity of the cold mass suspension (Z≈500 mm and 2500 mm). To complete the geometric survey, two further measurements are planned:

- Gap height measurements at cold conditions to prove that the coil itself is not restricting the gap height.

- Yoke gap measurements without coil.
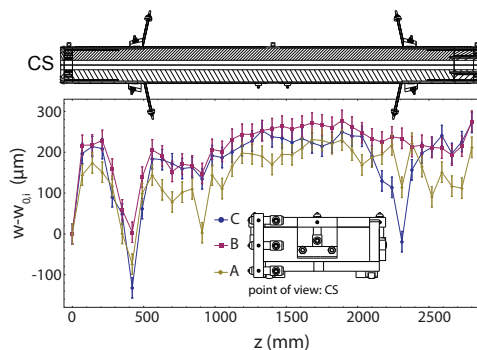
Figure 4: Measured gap width between coils.

FIELD ERROR ROOT CAUSES

Multiple simulations with ROXIE2D have been done to understand correlation between the manufacturing tolerance and magnetic field deviations. A 2D model of the magnet cross section based on the manufacturing drawings was established. Then, manufacturing tolerances were listed and the most probables introduced into the model. Some (exaggerated) examples are shown in Fig. 5.
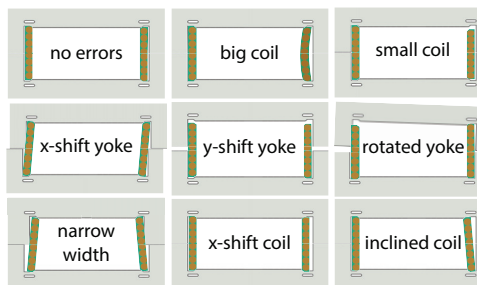
Figure 5: Examples of variation of manufacturing errors.

Several cases were simulated to reproduce the measured magnetic field deviation. For example, the "rotated yoke" case induces normal and skew quadrupole fields (gradient of B_x, as shown in Fig. 6). Qualitatively, this result confirmed the consistency between the results from the magnetic field measurements and gap height measurement. However, only considerably large manufacturing errors could explain the measured fields quantitatively. In this case, a difference in the gap parallelism of 165 μm was estimated contrary to the measured 80 μm.

So far, the measured field distortion could not be explained by only one manufacturing error in any of the studied cases. Therefore, multiple manufacturing errors are considered as a cause of the field distortion.

In addition, sensitivity of the manufacturing tolerances of the cable position and yoke geometry to multipole field error was investigated with Monte Carlo method. ±50 μm random errors were assumed to each cable position or four corners of the pole surface. In both cases, computations were repeated 500 times and delivered histograms of the multipole field coefficients. Figure 7 shows a summary of the standard deviation of the multipole field errors from the histograms.
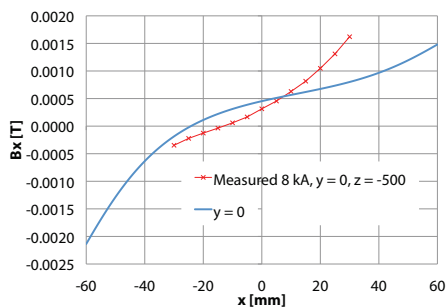
Figure 6: Measured and computed B_x.

Obviously the yoke geometry is more sensitive than the cable position to both normal and skew multipoles. The cable positions affects mainly skew multipole field. Consequently, the yoke geometry should be more strictly controlled as the cable position in the coil package during the manufacturing process.
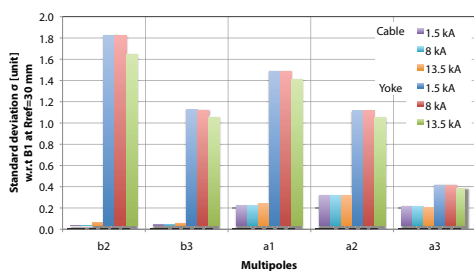
Figure 7: Standard deviation of multipole field coefficients with 500 times computation.

BEAM STABILITY

The measured harmonics from the FoS dipole have been taken as a base for simulations of the SIS100 dynamic aperture (DA). The systematic parts of the non-allowed components (b_2, b_4, b_6, a_n) have been set to zero, while the systematic parts of the allowed components (b_3, b_5, b_7) were taken from the FoS measurements. The random parts ($\sigma_{b,a}$) are given by the magnetic measurements with the known manufacturing tolerances taken into account. At the Non-Cable-Connection-Side (NCS), a replaceable yoke insert for end field optimization was installed which in reality disturbed the field more than the non-optimized end where no insert was installed. Therefore, in the reference model of the dipole as shown in Tab. 1, the NCS harmonic values have been replaced by the Connection-Side (CS) values.

The DA was calculated using the MAD-X code [11] and the minimum-stable single particle emittance algorithm [12]. The reference computer model of the main quadrupole magnets have been taken for the systematic and random multipole errors. Closed-orbit distortions Δx_{rms} =1.5 mm, Δy_{rms} =1 mm have been assumed, the total effects of the multipole errors on the betatron tunes and chromaticity have been compensated by the main quadrupole fields and corrector magnets.

Table 1: Dipole Harmonic Errors in Units (1×10^{-4}) and Standard Deviations for the DA-simulation

order n	b_n	$\sigma_{b,n}$	a_n	$\sigma_{a,n}$
1	1×10^4	0	0	0
2	0	2.95	0	1.06
3	-10.8	2.87	0	1.0
4	0	2.01	0	0.78
5	3.68	2.53	0	0.38
6	0	3.37	0	0.62
7	5.3	2.23	0	0.9

The main source of the tune spread in SIS100 high intensity beams is space charge, thus the scan has been performed along the line of the corresponding tune footprint. Particles have been tracked for 10^3 turns, which is conservative (the synchrotron period during the 1 s injection plateau is $\approx$100 turns).

Figure 8 shows the results of the DA scans for the SIS100 operation at $Q_{x,y}$ = 18.84, 18.73. The DA is shown in transverse emittance units, with ε = 35 mm mrad as the standard total (2σ) emittance. The value 3ε was considered as a sufficient safety margin. Two stop-bands with the zero DA correspond to the half-integer Q_y = 18.5 and the normal third-order resonance. For comparison, a model without the 6th and 7th order errors was computed (as those have large measurement uncertainties).
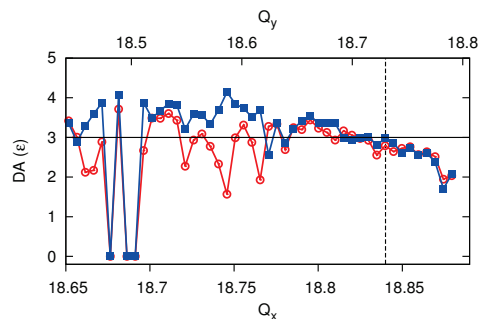
Figure 8: Simulated dynamic aperture. Red: complete dipole magnet model, blue: model without components of the 6th and 7th order.

MITIGATION STRATEGY

For the DA of SIS100, dominant are the systematic errors which result in large stop band widths. Therefore, the random components of a_2, b_4, a_3 have to be controlled tightly during the production. To accommodate this, a strategy was worked out with the dipole manufacturer to ensure good reproducibility of the yoke assembly. Special care was taken regarding the welding procedure (at the yoke suspension points, too). Gap parallelism, height and width will be held under tight control and measured during production.

REFERENCES

[1] H. Khodzhibagiyan, A. Kovalenko, A. Agapov, V. Alexeev, V. Drobin, A. Starikov, Yu. Shishov, N. Vladimirova, G. Moritz, E. Fischer, L. Potanina, A. Shikov, G. Vedernikov, and A. Kalimov. Design and test of new hollow high current NbTi cable for fast ramped synchrotron magnets. In *The 6th European Conference on Applied Superconductivity (EUCAS 2003)*, number 181 in Conference Series. Institute of Physics, 2004.

[2] E. Fischer, H. Khodzhibagiyan, A. Kovalenko, and P. Schnizer. Fast ramped superferric prototypes and conclusions for the final design of the SIS100 main magnets. *IEEE T. Appl. Supercon.*, 19(3):1087–1091, June 2009.

[3] Egbert Fischer, Hamlet Khodzhibagiyan, and Alexander Kovalenko. Full size model magnets for the FAIR SIS100 synchrotron. 18(2):260–263, June 2008.

[4] E. Fischer, P. Schnizer, P. Akishin, R. Kurnyshov, A. Mierau, B. Schnizer, S. Y. Shim, and P. Sherbakov. Superconducting SIS100 prototype magnets design, test results and final design issues. *IEEE T. Appl. Supercon.*, 20(3):218–221, June 2010.

[5] E. Fischer, P. Schnizer, A. Mierau, P. Akishin, and J. P. Meier. The SIS100 superconducting fast ramped dipole magnet. In *Proceedings of IPAC2014, Dresden, Germany*, 2014.

[6] E. Fischer, P. Schnizer, K. Sugita, J. P. Meier, A. Mierau, A. Bleile, P. Szwangruber, H. Müller, and C. Roux. Fast ramped superconducting magnets for FAIR – production status and first test results. *IEEE T. Appl. Supercon.*, 2014. submitted for publication.

[7] P. Schnizer, B. Schnizer, P. Akishin, and E. Fischer. Theory and application of plane elliptic multipoles for static magnetic fields. *Nuclear Instruments and Methods in Physics Research Section A: Accelerators, Spectrometers, Detectors and Associated Equipment*, 607(3):505 – 516, 2009.

[8] P. Schnizer, E. Fischer, H. Kiesewetter, F. Klos, T. Knapp, T. Mack, A. Mierau, and B. Schnizer. Commissioning of the mole for measuring SIS100 magnets and first test results. *IEEE T. Appl. Supercon.*, 20(3):1977–1980, June 2010.

[9] P. Schnizer, E. Fischer, P. Akishin, J. P. Meier, A. Mierau, and A. Bleile. Advanced magnetic field description and measurements on curved accelerator magnets. In *Proceedings of IPAC2014, Dresden, Germany*, 2014.

[10] P. Schnizer, B. Schnizer, and E. Fischer. Cylindrical circular and elliptical, toroidal circular and elliptical multipoles, fields, potentials and their measurement for accelerator magnet. *arXiv preprint physics.acc-ph*, October 2014.

[11] MAD-X Code: http://mad.home.cern.ch

[12] V. Kornilov, O. Boine-Frankenheim, V. Kapin, Proc. of IPAC2010, Kyoto, Japan, May 23-28, p. 1988 (2010)